

# Microstructural Elucidation of Self-Emulsifying System: Effect of Chemical Structure

Sharvil S. Patil • Edakkal Venugopal • Suresh Bhat • Kakasaheb R. Mahadik • Anant R. Paradkar

Received: 22 January 2012 / Accepted: 19 March 2012 / Published online: 4 April 2012  
© Springer Science+Business Media, LLC 2012

## ABSTRACT

**Purpose** Self-emulsifying systems (SES) emulsify spontaneously to produce fine oil-in-water emulsion when introduced into aqueous phase. The self-emulsification process plays an important role during formation of emulsion. The objective of current work was to understand and explore the inner structuration of SES through controlled hydration and further to study the influence of additive on the same which ultimately governs performance of final formulation in terms of droplet size.

**Methods** Droplet size of final formulations containing structural analogues of ibuprofen was determined. Microstructural properties of intermediate hydrated regimes of SES were investigated using techniques such as small angle X-ray scattering, differential scanning calorimetry and rheology.

**Results** The current work established inverse relationship between droplet size of the formulations containing structural analogues of ibuprofen and their Log P values. Microstructural analysis of intermediate hydrated regimes of the prepared samples showed formation of local lamellar structure. Structural analogues of ibuprofen significantly altered microstructure of lamellae which was well correlated with the droplet size of final formulations. *In vitro* drug release study showed increase in dissolution rate of lipophilic drugs when formulated as SES.

**Conclusion** The current work emphasizes the fact that tailor-made formulations can be prepared by controlling the properties of intermediate regimes.

**KEY WORDS** emulsion • flurbiprofen • ibuprofen • ketoprofen • lamellar structure • self-emulsifying system • structural analogues

## INTRODUCTION

Self-emulsifying drug delivery systems (SEDDS) are isotropic mixtures of oils and surfactants sometimes contain co-solvents or co-surfactant, which emulsify spontaneously to produce fine oil-in-water emulsions when introduced into aqueous phase under gentle agitation (1). The process of self-emulsification leading to formation of an emulsion has been the focus of research. Several attempts have been made to describe the mechanism governing process of self-emulsification (2,3). It has been reported that self-emulsification occurs when the entropy change that favors dispersion is greater than the energy required to increase the surface area of the dispersion (4). One of the mechanisms claimed by researchers to describe the process of self-emulsification involves formation of liquid crystal (LC) phase at the interface which ruptures upon successful penetration by water. The rate and extent of water penetration into intermediate gel phase (involving LC phase) formed during self-emulsification process will govern the droplet

S. S. Patil • K. R. Mahadik (✉)  
Dept. of Pharmaceutics, Bharati Vidyapeeth University  
Poona College of Pharmacy  
Erandwane  
Pune 411 038 Maharashtra, India  
e-mail: krmahadik@rediffmail.com

A. R. Paradkar (✉)  
Centre for Pharmaceutical Engineering Science  
University of Bradford  
West Yorkshire  
Bradford BD7 1DP, UK  
e-mail: a.paradkar1@bradford.ac.uk

S. S. Patil • E. Venugopal • S. Bhat  
Polymer Science and Engineering Division  
National Chemical Laboratory  
Pune 411 008, India

size of final oil in water emulsion (5–8). Thus in other words, ‘LC phase formation and its rupture’ can be regarded as droplet size (and in turn performance of the system) controlling step identical to ‘rate’ controlling step in progress of a specific reaction. In order to assess the rapid self-emulsification process, self-emulsifying system (SES) can be studied after controlled hydration. Our group has investigated viscoelastic properties of intermediate LC phase formed during self-emulsification process and its influence on droplet size of final formulation. It was observed that intermediate hydrations of system which presented higher viscous component formed emulsion with smaller droplets and vice a versa (9). Recently we have investigated effect of ions on mesophasic transformations (inner structuration) in SES and its effect on droplet size of final formulation. The work suggests that the properties of intermediate LC phase formed during self-emulsification process are altered by additive (10).

The objective of current work is to understand and explore the microstructural properties of hydrated intermediate regimes (involving intermediate gel phase) of SES consisting of non-ionic surfactants and further to investigate effect of additive on the inner structuration of hydrated intermediate regimes affecting the performance (droplet size) of final formulation. In the present work pharmaceutically permitted ingredients such as Captex® 355 (oil), Tween 80 (surfactant) and Capmul® MCM (CMCM, co-surfactant) were used to prepare SES. Microstructural properties of intermediate hydration regimes of prepared SES were studied in detail. Influence of structural analogues of ibuprofen (Fig. 1) on inner structuration of intermediate hydrated regimes and its effect on performance

in terms of droplet size of emulsion have been explored. Systems containing ketoprofen, ibuprofen and flurbiprofen (0.13M) were prepared. Microstructural properties of intermediate hydrated regimes of prepared SES were investigated using plane polarized light microscopy, small angle X-ray scattering (SAXS), rheology and differential scanning calorimetry (DSC). The formed emulsions were analyzed for droplet size and *in vitro* drug release study. The current work has been designed to understand the influence of mesophasic transformations on pharmaceutical performance of prepared SES.

## MATERIALS AND METHODS

### Materials

Captex® 355 (Caprylic/Capric Triglyceride), Capmul MCM (CMCM, Glyceryl mono- and dicaprate) were generous gift samples from Abitec Corporation, USA. Tween 80 (Polyoxyethylene 20 sorbitan monooleate) was purchased from Merck Chemicals, Mumbai, India. Ketoprofen, flurbiprofen and Ibuprofen were obtained as a generous gift from Glenmark Pharmaceuticals, FDC Limited, Mumbai and Torrent Pharmaceuticals, Gujrat respectively.

### Methods

#### Formulation of Plain SES (PSES)

PSES was formulated after screening of different ratios of Captex® 355 and Tween 80 in the range of 0–100% w/w. The optimized formula for PSES consisted of 40%w/w Captex® 355 and 60%w/w of surfactant (consisting of 40% w/w of Tween 80 and 20%w/w of CMCM).

#### Formulation of Drug-Loaded SES

Ketoprofen, ibuprofen and flurbiprofen (0.13 M) each was dissolved in PSES separately to obtain ketoprofen loaded SES (KSES) and similarly ISES, FSES respectively.

#### Hydration of SES

The prepared SES were hydrated at hydration levels in the range of 10–70% v/v with deionised water and stored for 24 h before analysis.

### Characterization

#### Emulsifying Properties

A fixed amount (40μL) of SES was added to 100 mL distilled water at  $25 \pm 0.5^\circ\text{C}$  and performance of

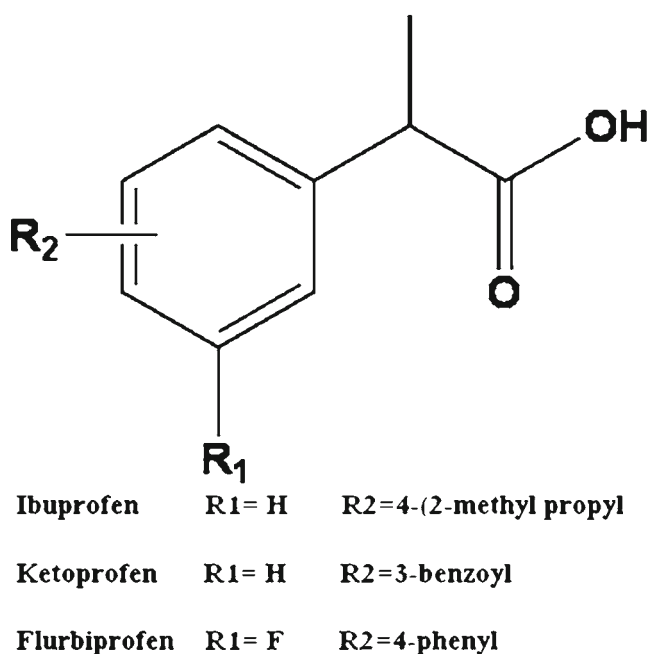


**Fig. 1** Chemical structure of ibuprofen, ketoprofen and flurbiprofen.

spontaneous emulsification was observed visually and analyzed according to droplet formation pattern (9). This test was performed in triplicate.

### Drug Content

Ketoprofen, ibuprofen and flurbiprofen from preweighed KSES, ISES and FSES respectively were extracted by dissolving in 25 mL methanol. Drug content in the extract obtained from KSES, ISES and FSES was analyzed spectrophotometrically at 259, 264 and 246 nm respectively.

### Droplet Size Measurement

Droplet size of all the prepared SES was measured by BIC 90 Plus Particle Size Analyser (Brookhaven Instruments Corporation, USA). For measurement, PSES was pre-diluted by addition of 0.5 mL of SES to 100 mL of distilled water under slow agitation at room temperature ( $25 \pm 0.5^\circ\text{C}$ ). Dynamic light scattering from the sample was used to determine hydrodynamic radius. KSES, ISES and FSES were analyzed using similar procedure. Analysis was done in triplicate.

### Rheological Studies

Rheological measurements of hydrated SES were performed using a controlled stress rheometer (Viscotech Rheometer, Rheologica Instruments AB, Lund, Sweden). Data analysis was done with Stress RheoLogic Basic software, version 5.0. A cone and plate geometry was used with 25 mm diameter and cone of  $1.0^\circ$ . Fresh sample was used for every test and all measurements were carried out at  $25 \pm 0.5^\circ\text{C}$ . Viscometry test was performed for intermediate hydrated samples (30–50% v/v) of PSES, KSES, ISES and FSES with shear stress varying in the range of 0.1–100 Pa.

### Polarized Light Microscopy

Plane polarized light microscopy of hydrated SES was performed for identifying the type of mesophase formed in the prepared sample (11). Hydrated SES was transferred to a specially fabricated glass tube (internal diameter 0.5 cm) and then viewed for presence or absence of birefringence under polarizing microscope at  $25 \pm 0.5^\circ\text{C}$  with  $\lambda/4$  compensator under 40X magnification (Nikon Eclipse E 600, Nikon Instech Co., Japan).

### Small Angle X-ray Scattering (SAXS) Studies

SAXS experiments were done on a Bruker Nanostar with rotating Cu anode and pinhole geometry. The instrument uses a copper  $K\alpha$  radiation of wavelength 1.54 Å. The

anode was operated with a current of 100mA and a potential difference of 45kV, and the sample to detector distance was 105 cm. The samples were taken in a quartz capillary of 2mm diameter and 10µm wall thickness. Background from an empty capillary was subtracted, after accounting for the sample absorption. A Bruker Peltier heating cooling unit was used for temperature control in the system. The data was collected on a HISTAR gas-filled multiwire detector and was circularly averaged to get a 1D curve. Scattering from intermediate hydrated samples of PSES, KSES, ISES and FSES was measured for long enough that the scattered intensity gave at least 3 million counts on the detector. Since we anticipate a locally lamellar structure, we use the Teubner Strey (T-S) model to analyze the SAXS data (12). Here,

$$I(q) = \frac{1}{a + bq^2 + cq^4} \quad (1)$$

where a, b and c are fitting parameters. The fitting constants can be used to determine the periodic domain spacing (d) and the correlation length ( $\xi$ ) by

$$d = 2\pi \left[ \frac{1}{2} \left( \frac{a}{c} \right)^{1/2} - \frac{1}{4} \left( \frac{b}{c} \right) \right]^{-1/2} \quad (2)$$

$$\xi = \left[ \frac{1}{2} \left( \frac{a}{c} \right)^{1/2} + \frac{1}{4} \left( \frac{b}{c} \right) \right]^{-1/2} \quad (3)$$

### Differential Scanning Calorimetry (DSC)

Calorimetric measurements were performed with Mettler Toledo 821e instrument equipped with an intracooler (Mettler Toledo, Switzerland).  $10 \pm 3$  mg of 45% v/v hydrated PSES, KSES, ISES and FSES sample was placed in closed aluminum crucibles separately and cooled to  $-30^\circ\text{C}$  at the rate of  $10^\circ\text{C}/\text{min}$ . They were maintained at  $-30^\circ\text{C}$  for 10 min and subjected to heating from  $-30$  to  $10^\circ\text{C}$  at the scanning rate of  $3^\circ\text{C}/\text{min}$ . To ensure accuracy of caloric data instrument was calibrated with Indium/zinc.

### In Vitro Drug Diffusion Studies

*In vitro* diffusion studies were carried out for KSES, ISES and FSES using dialysis technique in triplicate. One end of pretreated cellulose dialysis tubing (7 cm in length) was tied with thread and then 1 mL of KSES (equivalent to 30 mg ketoprofen) was placed in it along with 5 mL of dialyzing medium (distilled water). The other end of tubing was also secured with thread and was allowed to rotate freely in dissolution vessel of USP 24 type II dissolution test apparatus that contained 900 mL dialyzing media (distilled water)

maintained at  $37 \pm 0.5^\circ\text{C}$  and stirred at 100 rpm. Placebo formulation (PSES) was also tested likewise simultaneously under identical conditions so as to check interference, if any. Aliquots were collected periodically and replaced with fresh dialyzing medium. Aliquots, after filtration through Whatman filter paper (no. 41), were analyzed spectrophotometrically at 259 nm for ketoprofen content. Similar procedure was followed for *in vitro* drug diffusion study of ISES and FSES and the aliquots were analyzed spectrophotometrically at 264 and 246 nm respectively. The data was analyzed using PCP Disso v 3i software. The mechanism of drug release was estimated by fitting the dissolution data to Korsmeyer–Peppas equation (13).

$$M_t/M_\infty = kt^n \quad (4)$$

Where  $M_t$  represents the fraction of drug released in time  $t$  and  $M_\infty$  the amount of drug released after infinite time. The diffusional exponent of drug release ‘ $n$ ’ indicates the type of release mechanism during the dissolution process. For non-Fickian release, the  $n$  value falls between 0.5 and 1.0, while for Fickian diffusion,  $n=0.5$ .  $K$  represents a constant incorporating structural and geometrical characteristic of the device.

## RESULTS AND DISCUSSION

Self-emulsifying systems often contain medium chain triglycerides (MCT) as oil which keeps lipophilic guest molecules in solubilized form (14). In the present work Captex® 355, a MCT was selected as model oil. Non-ionic surfactant Tween 80 was used for preparing SES. Systems prepared with different ratios of Captex® 355: Tween 80 showed formation of stiff gel when diluted with water. Even vigorous shaking did not disperse the gel which forced the addition of cosurfactant in the system thereby introducing CCM as co-surfactant into the formulation. The tendency of spontaneous emulsification and appearance of formed emulsion were taken in consideration for optimizing the system containing ratio of oil: surfactant: cosurfactant. ‘Good’ emulsification was noted when droplets are formed spontaneously in water resulting in a transparent emulsion while it was noted as ‘moderate’ for spontaneous emulsification with milky appearance. Thus from preliminary studies we selected SES consisting of 40%w/w of Captex® 355 and 60%w/w surfactant mixture consisting of 40% w/w of Tween 80 and 20%w/w of CCM.

### Droplet Size Analysis

PSES along with drug loaded SES (KSES, ISES and FSES) were analyzed for droplet size distribution after

uncontrolled hydration (Fig. 2). The addition of drug molecule significantly reduced the droplet size of PSES ( $185.3 \pm 5.1$  nm) as analyzed by one way ANOVA followed by Dunnett multiple comparison test (Table I). Droplet size of KSES was found to be  $173.0 \pm 6.1$  nm ( $P < 0.05$ ) whereas that of ISES and FSES was found to be  $157.4 \pm 5.5$  nm and  $147.7 \pm 5.1$  nm ( $P < 0.01$ ) respectively. The order of reduction in droplet size was observed to be PSES > KSES > ISES > FSES. To investigate the changes associated with droplet size after addition of guest molecule we decided to elucidate microstructure of SES. The process of self-emulsification is rapid and therefore controlled hydration of prepared SES was done. The intermediate hydrations (30–50% v/v) of the prepared systems showed formation of gel phase which transformed into emulsion with subsequent increment in water and thus microstructure of this region has been elucidated in the present work.

The microstructural changes associated with intermediate gel phase after addition of drug molecule were analyzed using plane polarized microscopy, SAXS, rheology and DSC to understand its influence on droplet size of final formulation. Plane polarized microscopic analysis of hydrated samples of intermediate regime revealed complete optical isotropy i.e. absence of birefringence (11).

### Small Angle X-ray Scattering

The SAXS can be used as a tool to investigate inner structuration of colloidal systems (15–17). The extent of microstructural alteration of drug loaded SES in comparison to PSES was investigated by performing SAXS of samples from the intermediate hydrated regimes. The SAXS data generated from the samples was fitted with Teubner Strey equation for extracting periodic domain spacing  $d = (2\pi/k)$  and persistence length ( $\xi$ ) (12,18,19). We obtain a reasonable fit to SAXS data from ISES 30% v/v and 50% v/v

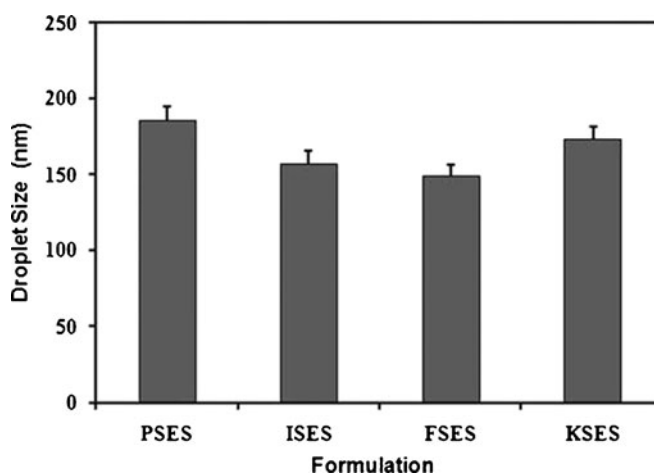


**Fig. 2** Droplet size analysis of various SES formulations ( $n=3$ ).

**Table 1** Droplet Size, Periodicity (d), Persistence Length ( $\xi$ ) and the Product  $k^*\xi$  Calculated from SAXS Measurements

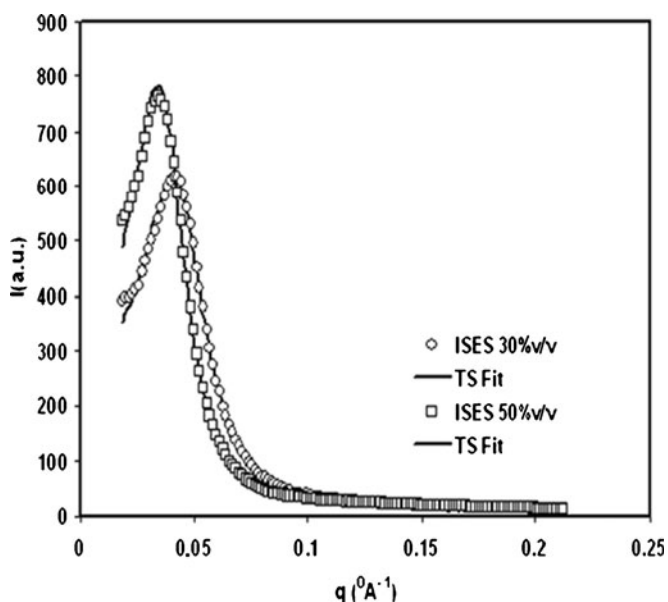
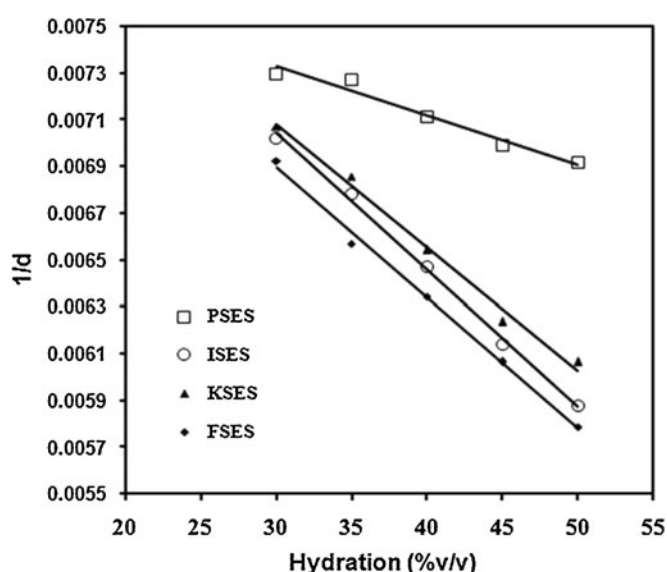
Sample	Log P (Pure Drug)	Droplet Size of Emulsion (nm) Mean $\pm$ SD	Hydration (%v/v)	d (Å°)	$\xi$ (Å°)	$k^*\xi$
PSES	—	185.3 $\pm$ 5.1	30	137	49.51	2.27
			35	137.46	63.63	2.91
			40	140.62	70.56	3.15
			45	143	72.79	3.20
			50	144.58	72.794	3.16
ISES	3.6	157.4 $\pm$ 5.5**	30	142.44	59.27	2.61
			35	145.45	60.19	2.60
			40	156.48	65.78	2.64
			45	165.78	67.03	2.54
			50	169.41	68.64	2.54
KSES	0.97	173 $\pm$ 6.1*	30	142.42	61.85	2.73
			35	145.83	63.51	2.74
			40	155.87	66.03	2.66
			45	162.33	69.02	2.67
			50	164.86	69.61	2.65
FSES	4.24	147.7 $\pm$ 5.1**	30	144.41	56.73	2.47
			35	154.92	63.54	2.57
			40	157.60	65.48	2.61
			45	164.86	68.13	2.60
			50	168.78	68.45	2.55

\*\*P < 0.01, \*P < 0.05 for Dunnett multiple comparison test

samples using the T-S model as shown in Fig. 3. Further the values of product  $k\xi$  ( $k$  obtained from  $d$ ) were found to be well above 2 (Table 1).

The microstructure associated with the intermediate hydrated regime was analyzed by constructing a plot of  $1/d$  versus hydration (%v/v). Construction of such plot showed linearity for all the samples from intermediate hydrated

regime (Fig. 4). Periodic domain spacing ( $d$ ) is measure of the quasi-periodic polar-nonpolar repeat distance. Figure 4 show that  $d$  value (Graph will be in reverse order) is highest for FSES whereas it is lowest for PSES. The order in which decrease in  $d$  value is observed can be represented as FSES > ISES > KSES > PSES.

**Fig. 3** Representative plot of Teubner Strey fit for ISES sample.**Fig. 4** Plot of  $1/d$  versus Hydration (%v/v) of intermediate hydrations of PSES, KSES, ISES and FSES.



The plot of persistence length ( $\xi$ ) versus hydration (%v/v) for the samples from intermediate hydrated regime is shown in Fig. 5. All the samples showed increase in persistence length with successive increment in water content. It can be observed that the persistence length was highest for PSES whereas it was lowest for FSES. The order of decrease in persistence length can be represented as PSES > KSES > ISES > FSES.

The dimensionality of swelling of microstructures can be readily obtained from the plot of  $1/d$  versus hydration (%v/v). One dimensional swelling shows linear plot as can be observed in Fig. 4 suggesting that the structures were well equilibrated in water. One dimensional swelling can be seen either in case of bicontinuous or lamellar structure. It has been well recorded that for bicontinuous microstructures the product  $k\xi$  falls in the narrow range between 1.5 and 2.0. All the samples from intermediate regime analyzed in the present work show values of the product  $k\xi$  well above 2.0, so it is unlikely that any bicontinuous structures form (20). Thus the data generated from the SAXS supports for existence of “local” lamellar structures. These structures are randomly oriented small stacks of layers in space but with local uniaxial behavior. These scattered fragments of lamellae are insufficient to show solution birefringent (21). Constantinides, P. P. *et al* have worked on similar system wherein they mention that the system used in the study shows large W/O and O/W microemulsion region. The regions have been identified using microscopy method. In the present work SAXS a powerful analytical tool has shown formation of lamellar structure in the system (22).

Log P values gives us an idea about the polarity of the molecule, higher the log P value more will be the nonpolar nature of the molecule. In the present work structural analogues used are ketoprofen, Ibuprofen and flurbiprofen

having log P value 0.97, 3.6 and 4.24 respectively (23,24). The polarity of molecule will govern its location within lamellae which in turn influence the microstructure formed within system. Thus ketoprofen will be located near the surfactant head group on account of its less nonpolar nature amongst the other two molecules whereas more nonpolar molecules will be located near the surfactant tails i.e. non-polar core of the lamellae (25). The lower values of  $d$  in case of PSES may be attributed to hydration of the hydrophilic polyoxyethelene (POE) chains of Tween 80 and their protrusion into the polar domain (water). Figure 4 shows increase in  $d$  values with increase in the log P values of the selected structural analogues. The increase in the  $d$  value with log P is believed to be due to dehydration of POE chains of surfactant. Such dehydration is induced by water repellent nature of the selected drug molecules which increased with log P. Thus system containing ketoprofen had lower  $d$  value than that of systems containing ibuprofen and flurbiprofen. Flurbiprofen has highest log P value, in other words highest nonpolar (hydrophobic) nature and thus might have dehydrated POE chains to a larger extent.

The stiffness of the surfactant/cosurfactant film can be better explained by using the persistence length: the shorter the persistence length the softer the film. PSES showed highest persistence length when compared to KSES, ISES and FSES indicating higher strength of surfactant/cosurfactant film. The process of hydration of POE chains is associated with hydrogen bond formation between oxygen atoms of POE groups and water which imparts strength to the surfactant/cosurfactant film. The nonpolar molecules might have hindered the process of hydration of POE groups and thus presented softer surfactant/cosurfactant film. The extent of hindrance to the hydrogen bond formation will be higher for FSES due to its high log P and minimum for KSES among the selected structural analogues. In case of PSES absence of nonpolar molecule did not disrupted the hydrogen bonds associated with atoms of POE groups and water thereby resulting in formation of stiff film. Systems with softer film might have presented lower resistance towards bending of surfactant film thus forming smaller droplets whereas reverse was the case for systems with stiffer surfactant film which might have shown high resistance towards bending and hence formed larger droplets during the process of self-emulsification. To support our assumption we also performed differential scanning calorimetric analysis of intermediate hydrated sample (45%v/v) of PSES, KSES, ISES and FSES.

### Differential Scanning Calorimetry

Subzero temperature differential scanning calorimetric study was used to elucidate microstructural changes occurring during the process of self emulsification. DSC can be used to probe the

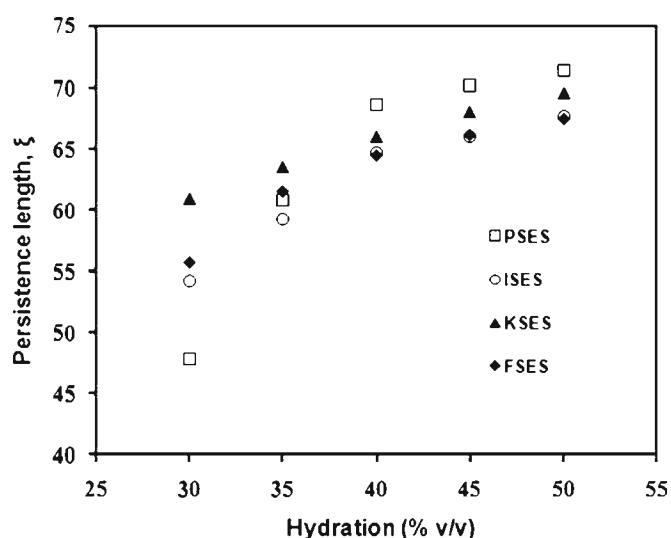


**Fig. 5** Plot of correlation length or persistence length ( $\xi$ ) versus hydration (%v/v) of intermediate hydrations of PSES, KSES, ISES and FSES.

thermodynamic property of water at subzero temperature levels. Depending on the position of melting endotherm in DSC thermogram water can be bound (which is associated to hydrophilic groups and melts below  $-10^{\circ}\text{C}$ ), interphasal water (defined as water confined within the interface of dispersed system, which melts at about  $-10^{\circ}\text{C}$ ) or free water which melts at  $\sim 0^{\circ}\text{C}$  (26–28). Figure 6 shows DSC thermogram of intermediate hydrated sample (45%v/v) of PSES, KSES, ISES and FSES. The endothermic events observed in DSC study have been listed in Table II. All the endothermic peaks were in the range of  $-5$  to  $-6^{\circ}\text{C}$  indicating that the water present in the system was interphasal water. However, FSES showed extra endothermic peak at about  $0^{\circ}\text{C}$  corresponding to free water.

The selected intermediate hydration of PSES, KSES, ISES and FSES was evaluated for degree of binding strength of water with the surfactant and drug by comparing the fusion temperatures and enthalpies of water. PSES and KSES showed endothermic peak at  $-5.67^{\circ}\text{C}$  and  $-5.15^{\circ}\text{C}$  with enthalpies  $-12.47\text{ Jg}^{-1}$  and  $-3.36\text{ Jg}^{-1}$  respectively. Thus there was drastic rise in the enthalpy (around 73%) when ketoprofen was introduced in the system. This suggests that the thermodynamic properties of water was altered in the presence of ketoprofen. In case of ISES and FSES the endothermic peak for melting of water was observed at  $-5.99$  and  $-5.19^{\circ}\text{C}$  with enthalpies  $-3.09$  and  $-1.03\text{ Jg}^{-1}$  respectively. The percent increase in enthalpy for ISES and FSES when compared to PSES was found to be 75% and 92% respectively. Thus the order of rise in the enthalpy can be represented as  $\text{FSES} > \text{ISES} > \text{KSES}$ . The stronger hydrophobic effect of flurbiprofen might have disrupted the structure of water to a larger extent when compared to ISES and KSES. The presence of endothermic peak for free water at  $0^{\circ}\text{C}$  with enthalpy  $-0.29\text{ Jg}^{-1}$  supports our assumption. Thus to summarize, thermodynamic properties

**Table II** Thermal Behavior of Systems at 45%v/v Dilution with Water

No.	Sample	Endothermic peak Temperature ( $^{\circ}\text{C}$ )		Enthalpy ( $\text{Jg}^{-1}$ )	
		Interphasal water	Free water	Interphasal water	Free water
1	PSES	$-5.67$	–	$-12.47$	–
2	KSES	$-5.15$	–	$-3.36$	–
3	ISES	$-5.99$	–	$-3.09$	–
4	FSES	$-5.19$	0	$-1.03$	$-0.29$

of intermediate hydration (i.e. hydration before transformation of the system into emulsion) of PSES, KSES, ISES and FSES were investigated using DSC. The absence of endothermic peak for free water in case of PSES, KSES and ISES indicated association of water molecules with the surfactant head groups. The presence of free water peak in case of FSES indicated its faster transformation towards emulsion with hydration whereas KSES and ISES did not show endothermic peak for free water which suggests that still the system had ability to accommodate the water in the system. Shear rheology can be used to investigate the microstructure of the system. In the present work we have analyzed rheological properties of intermediate hydrated regimes using viscometry studies.

## Rheology

The plot of shearing stress *versus* shear rate was constructed from the rheological data. The plot showed linearity over the entire screened range suggesting that the samples from the intermediate hydration regimes possess Newtonian flow (not shown). Figure 7 shows plot of viscosity *versus* hydration (% v/v) for intermediate regimes of PSES, KSES, ISES and FSES.

Rheological data supported swelling of intermediate microstructures as probed by SAXS and DSC since all the samples showed increase in the viscosity with hydration. It has been well documented that progressive hydration of surfactant headgroups enhances their mobility as probed from NMR studies. This entropy driven process leads to progressive loosening-up of the headgroup packing (29). Thus the increased mobility of surfactant might have led to loosening of the boundaries by the adjacent fluid lamellae thus interfering with each other. This process ultimately raised the viscosity of the analyzed systems with successive increment in water (30). The viscosity of PSES was highest whereas that of FSES was lowest within different samples screened by rheology. The order of reduction in viscosity by hydration can be represented by  $\text{PSES} > \text{KSES} > \text{ISES} > \text{FSES}$ . PSES did not hinder the hydration of surfactant head

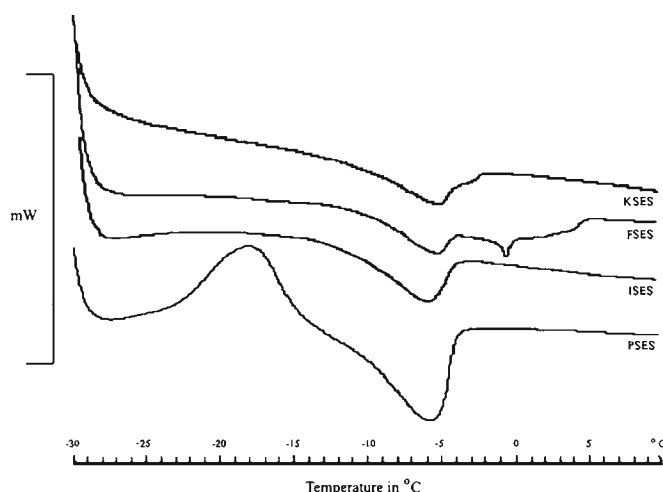


**Fig. 6** DSC thermogram of intermediate hydrated sample (45%v/v) of PSES, KSES, ISES and FSES.

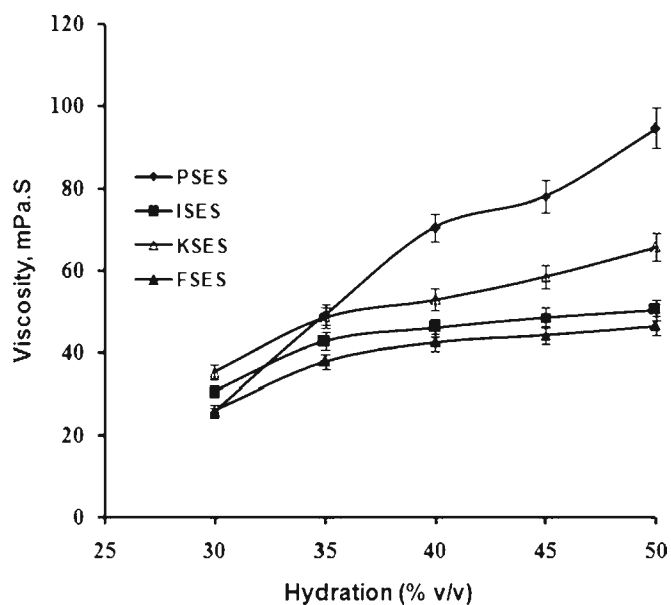


**Fig. 7** Plot of viscosity versus hydration (% v/v) for intermediate regimes of PSES, KSES, ISES and FSES ( $n=3$ ).

groups and thus showed highest viscosity. Amongst KSES, ISES and FSES, lowest viscosity associated with FSES was attributed to stronger hydrophobic nature of flurbiprofen which affected the degree of binding of water molecules to POE groups of surfactant whereas ketoprofen being less nonpolar showed highest viscosity suggesting its lower hindrance towards hydration of POE chains of the surfactant. Thus rheological studies well supported the results obtained by SAXS and DSC.

### In Vitro Drug Release Study

The type of mesophase formed upon hydration of lyotropic liquid crystals has been shown to govern drug release (31). The present work highlights effect of additive (drug) on microstructure of SES which in turn governs the droplet size of the final formulation. *In vitro* drug release study can be used as tool to assess performance of the prepared formulations. Thus drug release study for ketoprofen, ibuprofen and flurbiprofen was performed in distilled water where solubility for these drugs was limiting parameter. Dissolution rate was found to be increased in case of all the lipophilic drugs under consideration when formulated into SES (Fig. 8). Such improvement in dissolution rate in case of all the prepared formulations may be attributed to the smaller droplet size presented by them for effective dissolution and also wetting of drug promoted by the surfactants (32). The values of  $n$  extracted by fitting the dissolution data to Korsmeyer-Peppas equation lied between 0.7 and 0.9 for all drug loaded SES indicating that the drug release was following non-Fickian drug release kinetics.

## CONCLUSION

The present work explored microstructural properties of intermediate gel phase of SES and its influence on droplet size of final formulation. Microstructural properties of intermediate hydration regimes were investigated using SAXS, DSC and rheology. SAXS studies indicated formation of local lamellar structure within the intermediate hydration regimes which transformed into emulsion with subsequent hydration. The swelling of lamellar structure formed within the intermediate hydration regime was probed by DSC and rheology. In the present study effect of structural analogues of ibuprofen on microstructure of intermediate regime and its influence on performance (droplet size) of the final formulation has been investigated. Inverse relationship between  $\log P$  of drug molecule and droplet size was established. Thus to conclude, the nature of additive strongly influence the properties of the intermediate local lamellar structures formed during self emulsification process which ultimately affects the performance of the system. The current studies suggests that tailor-made formulations can be prepared if one can control the properties of the intermediate regimes.

## ACKNOWLEDGMENTS & DISCLOSURES

The authors thank Dr. Guruswamy Kumaraswamy, Scientist, Polymer Chemistry, National Chemical Laboratory for providing facility of Small Angle X ray Scattering and for extending his cooperation in SAXS data analysis and discussion.

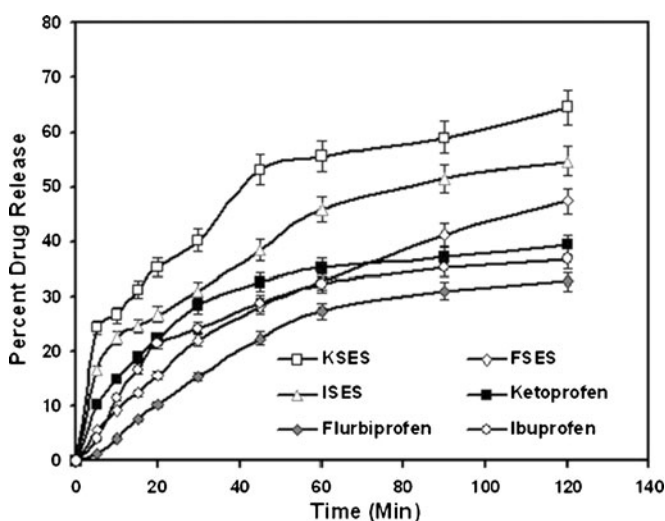


**Fig. 8** *In vitro* drug release profiles of ketoprofen, ibuprofen, flurbiprofen and SES formulations of the same ( $n=3$ ).



## REFERENCES

- Charman S, Charman W, Rogge M, Wilson T, Pouton C. Self-emulsifying drug delivery systems: formulation and biopharmaceutical evaluation of an investigational lipophilic compound. *Pharm Res*. 1992;9:87–93.
- Pouton C. Lipid formulations for oral administration of drugs: nonemulsifying, self-emulsifying and 'self-microemulsifying' drug delivery systems. *Eur J Pharm Sci*. 2000;11:S93–8.
- Pouton C, Porter C. Formulation of lipid-based delivery systems for oral administration: materials, methods and strategies. *Adv Drug Deliv Rev*. 2008;60:625–37.
- Reiss H. Entropy induced dispersion of bulk liquids. *J Colloid Interface Sci*. 1975;53:61–70.
- Groves M, De Galindez D. The self-emulsifying action of mixed surfactants in oil. *Acta Pharm Succ*. 1976;13:361–72.
- Wakerly M, Pouton C, Meakin B. Evaluation of the self-emulsifying performance of a non-ionic surfactant-vegetable oil mixture. *J Pharm Pharmacol*. 1987;39:6–10.
- Craig D, Barker S, Banning D, Booth S. An investigation into the mechanisms of self-emulsification using particle size analysis and low frequency dielectric spectroscopy. *Int J Pharm*. 1995;114:103–10.
- Rang M, Miller C. Spontaneous emulsification of oils containing hydrocarbon, non-ionic surfactant, and oleyl alcohol. *J Colloid Interface Sci*. 1999;209:179–92.
- Biradar S, Dhumal R, Paradkar A. Rheological investigation of self-emulsification process. *J Pharm Pharm Sci*. 2009;12(1):17–31.
- Patil S, Venugopal E, Bhat S, Mahadik K, Paradkar A. Probing influence of mesophasic transformation in self-emulsifying system: effect of ion. *Mol Pharm*. 2012;9(2):318–24.
- Rosevear F. The microscopy of the liquid crystalline neat and middle phases of soaps and synthetic detergents. *J Am Oil Chem Soc*. 1954;31:628–39.
- Teubner M, Strey R. Origin of the scattering peak in microemulsions. *J Chem Phys*. 1987;87(5):3195–200.
- Korsmeyer R, Gurny R, Doelker E, Buri P, Peppas N. Mechanisms of solute release from porous hydrophilic polymers. *Int J Pharm*. 1983;15(1):25–35.
- Pouton C. Formulation of self emulsifying drug delivery system. *Adv Drug Deliv Rev*. 1997;25:47–58.
- Glatter O, Strey R, Schubert K, Kaler E. Small-angle scattering applied to microemulsions. *Ber Bunsen-Ges Phys Chem*. 1996;100:323–35.
- Glatter O, Orthaber D, Stradner A, Scherf G, Fanun M, Garti N, Clement V, Leser M. Sugar-Ester nonionic microemulsion :structural characterization. *J Colloid Interface Sci*. 2001;241:215–25.
- Salonen A, Muller F, Glatter O. Dispersions of internally liquid crystalline systems stabilized by charged disklike particles as pickering emulsions: basic properties and time-resolved behavior. *Langmuir*. 2008;24(10):5306–14.
- Chen S, Chang S. Structural evolution of bicontinuous micro-emulsions. *J Phys Chem*. 1991;95:7427–32.
- Bauer C, Bauduin P, Diat O, Zemb T. Liquid interface functionalized by an ion extractant: the case of Winsor III microemulsions. *Langmuir*. 2011;27(5):1653–61.
- Regev O, Ezrahi S, Aserin A, Garti N, Wachtel E, Kaler E, Khan A, Talmon Y. A study of the microstructures of a four component non-ionic microemulsion by cryo TEM, NMR, SAXS and SANS. *Langmuir*. 1996;12:668–74.
- Cabos C, Marignan D. Local lamellar structure in dense micro-emulsions. *J Phys Rev B*. 1988;37:9796–9.
- Constantinides P, Scalart J, Lancaster C, Marcello J, Marks G, Ellens H, Smith P. Formulation and intestinal absorption enhancement evaluation of water-in-oil microemulsions incorporating medium-chain glycerides. *Pharm Res*. 1994;1(10):1385–90.
- Beetge E, Plessis E, Muller D, Goosen C, Rensburg F. The influence of the physicochemical characteristics and pharmacokinetic properties of selected NSAID'S on their transdermal absorption. *Int J Pharm*. 2000;193:261–4.
- Li Q, Tsuji H, Kato Y, Sai Y, Kubo Y, Tsuji A. Characterization of the transdermal transport of flurbiprofen and indomethacin. *J Contr Release*. 2006;110:542–56.
- Sinko P. Colloids. Physical pharmacy. 5th ed. New Delhi: Wolters Kluwer Health (India) Pvt. Ltd; 2007. p. 488–9.
- Senatra D, Lendinara L, Giri M. W/O microemulsions as model systems for the study of water confined in microenvironments: Low resolution  $^1\text{H}$  magnetic resonance relaxation analysis. *Progr Colloid Polymer Sci*. 1991;84:122–8.
- Ezrahi S, Aserin A, Fanun M, Garti N. Subzero temperature behaviour of water in microemulsions. In: Garti N, editor. Thermal behaviour of dispersed systems: surfactant science series, Vol. 93. New York: Marcel Dekker; 2001. p. 59–120.
- Kogan A, Shalev D, Raviv U, Aserin A, Garti N. Formation and characterization of ordered bicontinuous microemulsions. *J Phys Chem B*. 2009;113:10669–78.
- Ulrich A, Watts A. Molecular response of the lipid headgroup to bilayer hydration monitored by  $^2\text{H}$ -NMR. *Biophys J*. 1994;66:1441–9.
- Mezzenga R, Meyer C, Servais C, Romoscanu A, Sagalowicz L, Hayward R. Shear rheology of lyotropic liquid crystals: a case study. *Langmuir*. 2005;21(8):3322–33.
- Negrini R, Mezzenga R. pH-responsive lyotropic liquid crystals for controlled drug delivery. *Langmuir*. 2011;27:5296–303.
- Patil P, Joshi P, Paradkar A. Effect of formulation variables on preparation and evaluation of gelled self emulsifying drug delivery system of Ketoprofen. *AAPS PharmSci*. 2004;5(3):1–8.